The Role of Climatological State on Driving US Heat Waves Through Rossby Waves Packets

Valentina Castaneda[1] and Lei Wang[1]

[1]Purdue University

April 30, 2023

Abstract

While heat waves are local extreme weather events, a planetary Rossby wave pattern is statistically related to the occurrence of heat waves events in the U.S. However, whether such planetary wave patterns cause the enhanced statistics of local heat waves or as a coincidence is debatable. In this work, we hypothesize that the atmospheric climatological state dictates the slowly propagating wave pattern, which sets up a conducive large-scale environment for local US heat waves. We implement an idealized dry dynamic core model with an iterative approach to simulate the realistic North American summer climatological state. As the model can generate similar large-scale planetary wave patterns propagating throughout North America, significantly more heatwaves are generated, and the statistics of heat waves become consistent with that estimated in reanalysis products. The slowly propagating Rossby wave packets with a timescale of 20-30 days can serve as a new source of intraseasonal predictability.

The Role of Climatological State on Driving US Heat Waves Through Rossby Waves Packets

Valentina Castañeda[1], **Lei Wang**[1]

[1]Department of Earth, Atmospheric, and Planetary Sciences, Purdue University

Key Points:

- The climatological state drives the stationary Rossby wave propagation providing critical dynamical conditions for heat waves in the US.
- A dry atmospheric model with a corrected climatological state generates heatwaves that are statistically consistent with observations.
- The slowly propagating Rossby wave packets with a timescale of 20-30 days can be a source of intraseasonal predictability.

Corresponding author: Lei Wang, `leiwang@purdue.edu`

Abstract

While heat waves are local extreme weather events, a planetary Rossby wave pattern is statistically related to the occurrence of heat waves events in the U.S. However, whether such planetary wave patterns cause the enhanced statistics of local heat waves or as a coincidence is debatable. In this work, we hypothesize that the atmospheric climatological state dictates the slowly propagating wave pattern, which sets up a conducive large-scale environment for local US heat waves. We implement an idealized dry dynamic core model with an iterative approach to simulate the realistic North American summer climatological state. As the model can generate similar large-scale planetary wave patterns propagating throughout North America, significantly more heatwaves are generated, and the statistics of heat waves become consistent with that estimated in reanalysis products. The slowly propagating Rossby wave packets with a timescale of 20-30 days can serve as a new source of intraseasonal predictability.

Plain Language Summary

Heatwaves are the leading weather-related killer in the United States and affect mainly the most vulnerable communities. These extreme events are statistically related to a large-scale wave pattern of Rossby waves that features a zonal wavenumber five structure. To find out what controls this wave pattern, we use a simple general circulation model that only contains dry dynamics without complicated interactions with moisture or clouds. We found that by modifying the climatological state of temperature and velocity fields based on the observed structure from the Northern Hemisphere summer, we can observe the same wave number five pattern developing days before the heatwave events, resembling that from the observations. This result suggests that the climatological state of the Northern Hemispheric summer provides a conducive environment for heatwaves in the U.S. due to the slowed-down propagation speed of the Rossby wave packets. A deeper understanding of its dynamics is crucial because, as this pattern develops up to 20 days ahead of the extremes, the underlying physical process governing this pattern may serve as a source of predictability on the Subseasonal-to-Seasonal (S2S) timescale, a current gap of forecasts between weather and climate.

1 Introduction

Over the coming century, climate change is expected to increase average summer temperatures and the severity of extreme heat linked with heat waves events. In the United States, the frequency, intensity, and duration of heat waves have been increasing rapidly in recent decades, and this behavior is projected to continue in the next decades (Meehl & Tebaldi, 2004). Currently, forecasters in the United States can only predict extreme events up to 10 days in advance because, unlike in the tropics, circulation in the mid-latitudes is more chaotic as it is dominated by climatic noise (Feldstein, 2000).

However, it is intriguing to hypothesize that certain atmospheric circulation states can be substantially more predictable than the average scenario, because these circulation regimes are associated with low-frequency patterns (Schubert et al., 2011). With this in mind, and considering that different studies have suggested that propagating stationary Rossby Waves play an important role in the mid-latitude atmospheric variability, the scientific community recently has increased interest in the connection between extreme weather events and large-scale atmospheric patterns such as Rossby Wave Packets (Chen & Newman, 1998; Schubert et al., 2011; Fragkoulidis & Wirth, 2020).

In many of the investigated cases, the extreme weather was linked to an upper-tropospheric trough (i.e., a breaking Rossby Waves). For example, Chen and Newman (1998) suggests that Rossby Waves originating in the west Pacific were the key in initiating intense anomalous anticyclones during the 1988 U.S. drought. Also, Schubert et al. (2011) relates this large-scale pattern with monthly mean precipitation and surface temperature variability over many regions of the extratropical land areas, including the northern U.S., parts of Canada, Europe, and Russia. Following the same approach, Ding and Wang (2005) found an interannually varying Northern Hemisphere circumglobal pattern with a preferred wavenumber five structure. This particular structure is confined within the waveguide associated with the summer north jet stream in the stationary state and is linked to significant surface air temperature and rainfall anomalies in western Europe, European Russia, India, East Asia, and North America. In a more recent study Teng et al. (2013), more concrete evidence has been shown of the relationship between the occurrence of heatwaves in the U.S. and the same wavenumber five pattern developing as early as 20 days ahead of the events. Despite the growing evidence for the concurrences of this interesting wave number five pattern, the physical mechanism that drives the atmospheric pattern and thus determines heatwaves has yet to be understood.

This study aims to understand better the fundamental role of atmospheric dynamics in the evolution of U.S. heat waves based on the hypothesis that the climatological state for the Northern Hemisphere summer drives the stationary Rossby wave propagation providing critical dynamical conditions for heat waves in the U.S. Inspired by the motivation to look for the simplest possible model in the climate model hierarchies (Held, 2005), we adopt an idealized dry dynamical core that allows for a bias correction of the mean flow structure without physical parameterizations. This approach allows us to isolate the role of intrinsic planetary waves in the evolution of extreme events.

2 Data and Methods

2.1 Reanalysis products

For the observational analysis, the NCEP/NCAR reanalysis of the National Oceanic and Atmospheric Administration (NOAA) was implemented. The surface air temperature (SAT), all levels of temperature and the meridional and zonal components of the wind at 300 hPa (V_{300} and U_{300}) were obtained from these databases with a spatial resolution of 2.5° and daily temporal resolution from 1948 to 2023.

2.2 An Idealized GCM with realistic climatological basic state

Idealized general circulation models are commonly used for the study of atmospheric dynamics. A dry dynamical core model solves the primitive equations on the sphere by nudging the climatological temperature field toward a prescribed structure of radiative equilibrium temperature (T_{eq}). Essentially, this process isolates the dry atmospheric dynamics from the complex physical parameterizations.

We use the open-access updated version from (Wu & Reichler, 2018) of the spectral dynamical core model proposed by (Held & Suarez, 1994) for the Geophysical Fluid Dynamics Laboratory (GFDL). The model has a horizontal resolution of T42 (64x128 grid) and 40 vertical σ levels between the surface and 0.01 hPa. To represent the boundary-layer friction, Rayleigh drag is used to remove momentum in the lower troposphere between the surface and $\sigma = 0.7$. By default configurations of this model, the temperature is forced by Newtonian relaxation toward a prescribed equilibrium temperature as follows:

$$\frac{\partial T}{\partial t} = \frac{T - T_{eq}}{\tau} \tag{1}$$

where τ is the prescribed relaxation timescale.

Since the primary purpose of this study is to examine how the atmospheric basic state controls the large-scale Rossby Wave pattern with a zonal wavenumber five struc-

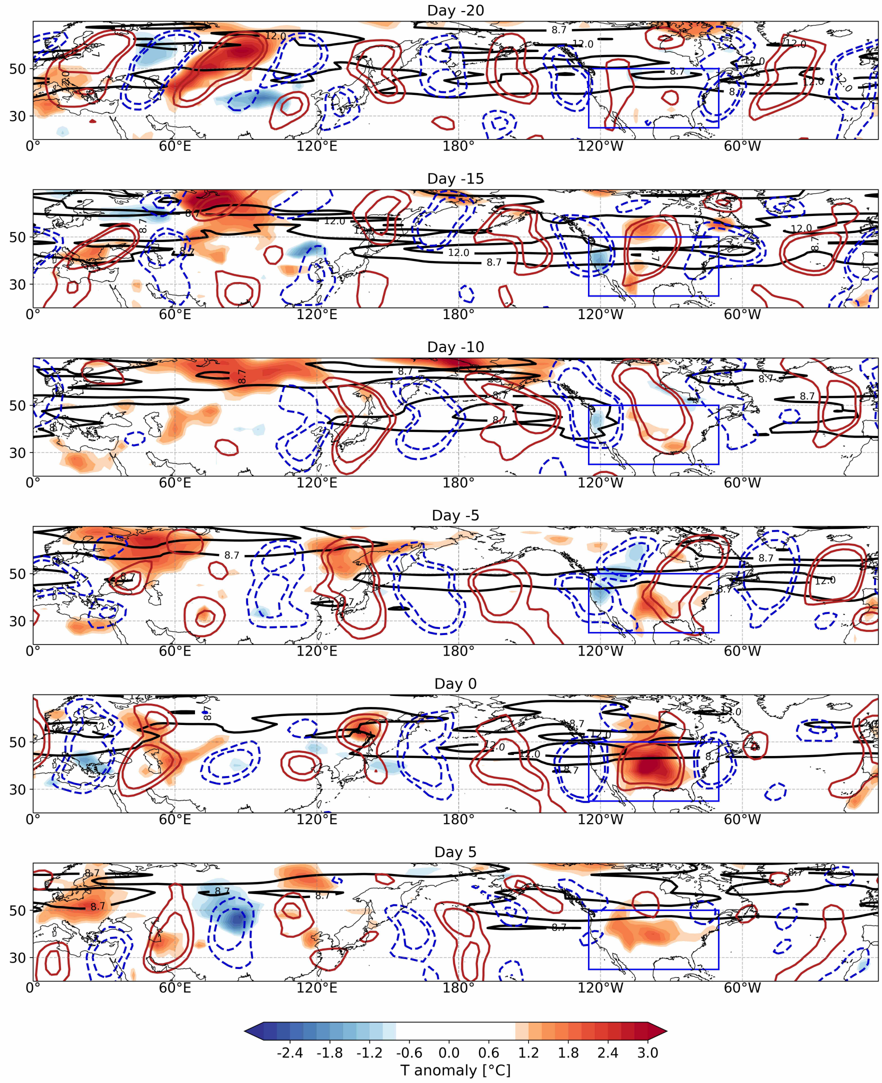

Figure 1. Evolution of heat waves 20 days ahead of the events: Red and dashed blue contours represent composites of 200hPa streamfunction anomalies at ± 0.05, 0.08 (red as positives). Shading represents surface air temperature anomaly and black contours represent the Rossby Wave Packet envelope at levels 8.7, 12 m/s.

ture driving local heat waves in the US, the model includes the iterative procedure proposed by Chang (2006) to simulate the climatological basic state of the atmosphere in the idealized model. This consists of iterating the radiative equilibrium temperature profile so that at the end of the iterations, the model climate closely resembles the desired target climate (see Supporting Information for more details of the methodology). The iteration uses a fixed equilibrium temperature for each N step (T_{eq}) in a run of 62 years, for a total of 21630 days after eliminating the first 1000 days of simulation. Then, we calculate the model simulated temperature climatology $T_{(N)}$ and correct it concerning basic state from the NCEP reanalysis data T_R. The next iteration step N+1 is calculated according to:

$$T_{eq(N+1)} = T_{eq(N)} - \frac{2}{3}(T_{(N)} - T_R), N = 1, 2, 3... \tag{2}$$

To assess the role of the climatological basic state, we carry out three experiments as follows:

- **Held and Suarez 1994 configuration (CTR)**: the zonal-mean temperature structure is relaxed toward a prescribed equinoctial radiative-equilibrium state. It's the default configuration described in detail in (Held & Suarez, 1994) and leads to a climatological state close to the observed annual mean climatological state.
- **Zonally-symmetric boreal summer (ZOB)**: The ratiative forcing T_R described in section 2.2 and in eq. 2 is set by the two-dimensional (i.e., latitude-pressure) basic state from the NCEP reanalysis data. For this experiment, we use the zonally symmetrical distribution of temperature for the climatological boreal summer (June, July, and August) between 1948 and 2021.
- **Realistic Northern Hemisphere summer (ROB)**: The full three-dimensional structure of the radiative forcing T_R is obtained from the climatological boreal summer from NCEP, especially including zonal asymmetries. This bias correction includes zonal variations in T_{eq}, which can be related to zonal variations in diabatic heating as discussed in Chang (2006) work.

2.3 Heat waves identification

A heatwave event is set as at least five consecutive days with more than around 900000 km^2 over the US continental area (125W – 70W, 25N – 50N) with daily averaged SAT exceeding a threshold value, and the center of these warm points, considered as the point of maximum temperature, does not move faster than 5 latitude or longitude per day. The temperature threshold varies spatially as well as with the day of the year. It was established as the percentile 97.5 of the historical SAT. This approach follows Teng et al. (2013).

2.4 Rossby Wave Packets evolution

As this study aims to understand the dynamics behind heat waves, it is necessary to look at the evolution of the Rossby Waves Packets driving extreme events from observational data and modeling outputs. Both the eddy phase speeds and their group velocity are important physical properties of Rossby Wave Packets' propagation. In particular, the eddy phase speed indicates the propagation speed of individual troughs within Rossby Waves Packets. It can thus be critical for the persistence of extreme surface weather (Röthlisberger et al., 2019). On the other hand, the group velocity reflects how quickly the whole packet propagates locally and represents the rate at which the Rossby waves transfer energy horizontally (Pedlosky, 2003). Based on the Rossby Waves Packets' progression in longitude and time, we compute the envelope of the meridional wind indicating their preferred regions of formation and decay. Specifically, we estimate the Rossby

Waves Packets' propagation by constructing Hovmöller diagrams using streamfunction anomalies at 300 hPa and the corresponding Rossby Waves Packets' envelope.

Subsequently, we calculate the local (in space and time) group velocity using the Rossby Waves Packets' envelope, which reflects how the flow features of enhanced meridional wind amplitude propagate in the zonal and meridional directions (Fragkoulidis & Wirth, 2020). We implemented the method proposed by Zimin et al. (2003) for the calculation of Rossby Waves Packets' envelope involving the Hilbert transform along circles of constant latitude combined with a restriction of the zonal wavenumber to a specified interval, which in this case corresponds to wavenumbers between 3 and 11. We implement this methodology using the meridional wind, which is usually implemented for the diagnosis of meridional deviations from the zonal flow, and is particularly well suited for the detection of Rossby waves. Specifically, we take the upper-tropospheric (300 hPa) meridional wind which features strong Rossby Waves Packet's activities (Wirth et al., 2018). The meridional wind anomaly $v(x)$ is considered on an equidistant grid along a latitude circle, where $x = 2\pi/N$ with $0 < x \leq 2\pi$, N is an even integer, and $l = 1, 2, ..., N$. The Fourier transform of the real function $v(x)$ is computed as:

$$\hat{v}_k = \frac{1}{N} \sum_{l=1}^{N} v\left(\frac{2\pi l}{N}\right) e^{-2\pi i k/N}, \left(K = -\frac{N}{2} + 1, ..., \frac{N}{2}\right) \tag{3}$$

The inverse Fourier transform is applied to a selected band of the positive wavenumber half of the Fourier spectrum:

$$w\left(\frac{2\pi l}{N}\right) = 2 \sum_{k=k_{min}}^{k_{max}} \hat{v}_k e^{2\pi i k/N} \tag{4}$$

Finally, the packet envelope is calculated as follows:

$$A(2\pi l/N) = |w(2\pi l/N)| \tag{5}$$

3 Results

3.1 Stationary waves preceding heat waves in reanalysis

From the reanalysis data, we found 165 heat waves days from 26 events found in the 75 summers from NCEP. We look at the temporal evolution of the planetary waves preceding the events by constructing composites from day -20 to day 5 (Figure 1), where we designate the first day of a heatwave as day 0. We used daily sub-seasonal anomalies at 300 hPa streamfunction calculated as the daily departures from the long-term mean and from the seasonal (June-July-August) mean of the particular year. These anomalies were spatially filtered, considering only wavelengths between 2800 km and 10000 km to consider only the wavenumbers of interest and avoid noise. Defined low and high-pressure centers can be seen moving slowly westward, expected behavior for Rossby Wave propagation in the days leading up to the extreme event. Although several of the troughs and ridges are clearly seen, it cannot be readily determined whether the wavenumber is 5 or 6. This difficulty may be explained by the scarcity of the events in the reanalysis, which are rare by definition. On the other hand, the Rossby Waves amplitudes shown by the envelope reflect the energy transport by the propagating waves. Notably, the large amplitudes of the envelope are seen in the two ocean basins, consistent with the zones where the Rossby Waves tend to reach large amplitudes and phase speeds. (Fragkoulidis & Wirth, 2020).

3.2 Climatology on the idealized simulations

We first discuss the climatological circulation characteristics obtained for the 21630 analyzed days in each experiment (See Supporting Information Figures S1. and S2). As we used a prescribed temperature from NCEP reanalysis data for the Newtonian relaxation in the model, the bias-corrected experiments resemble the zonally symmetric and asymmetric Northern Hemispheric summer in the real atmosphere by construction. It means the temporal mean of the spatial distribution of the temperature, the barotropic averaged zonal wind, and the vertical distribution of the zonal wind, in general, resemble the atmosphere. It should be clarified that although some features of the corrected climatological state are not realistic, especially in the vertical distribution, they are realistic for the key latitudes of interest in this work (between 30°N and 60°N). Note that the basic atmospheric state of the CTR differs spatially and in magnitude from the real atmosphere. While in the real atmosphere, the peak jet intensity is about 10 m/s during the winter, the CTR exhibits a peak of more than 20 m/s. This is because the T_{eq} in the initial configuration is set based on annual climatology values rather than summer seasonality.

The expected phase speeds corresponding to the climatological zonal winds are calculated for different wavenumbers and compared to the results from reanalysis for the boreal summer (Figure 2). This is to elucidate the expected stationarity for the wave tracks preceding the events. The wavenumbers 5 and 6 have phase speeds close to zero for both observations and the bias-corrected experiments ZOB and ROB. From this calculation, we expect that any pattern associated with any of these wavenumbers can be developed before the events in the corrected experiments. However, the wavenumber five tends to precede U.S. heat waves (Teng et al., 2013). Although in this result for NCEP, it is wave number 6 that has phase velocity closest to 0, it should be noted that although the Rossby wave dispersion relation delves into the large-scale dynamics of mid-latitudes, it is based on a linearized approximation of the equations of motion, and may not accurately represent the behavior of atmospheric waves in situations where nonlinear interactions and other complicating factors are important. On the other hand, the overly strong eddy phase speed obtained for the CTR run again reflect the unrealistic climatology compared to the boreal summer, which provides a non-favorable large-scale environment for developing surface heatwaves. This explains the scarcity of heatwaves in the CTR.

3.3 Heat Waves driven by Intrinsic Planetary Wave pattern

Now that the model resembles the atmospheric basic state for the boreal summer, we can test our hypothesis that the basic state drives the stationary Rossby Waves propagation hence determining heat waves in the mid-latitudes. We must answer, firstly, if it resembles the actual statistics of heat waves, and secondly, if it resembles the atmospheric pattern preceding the events.

We compared the probability of heat waves days and the probability distribution function (PDF) of the events between the experiments and NCEP (Figure 4). We found 111 events and 765 heat waves days in the bias-corrected symmetrical case and 65 and 464 heat waves days in the asymmetric one. Both bias-corrected experiments resemble the PDF of the duration of the events in the reanalysis. However, only the one considering asymmetries (ROB) has a probability of occurrence of heat waves days similar to that found in the reanalysis. In contrast, the overly strong jetstream in the CTR run experiment can explain the extremely rare of similar heatwaves (only 5 events); the phase speeds of troughs are too high to drive persistent weather conditions. Indeed, by changing the detection methodology for this experiment, we can find slightly more events in the CTR. For example, considering a lower velocity of the center of the warm points or a minimum duration of the events shorter than five days, as shown in (Jiménez-Esteve

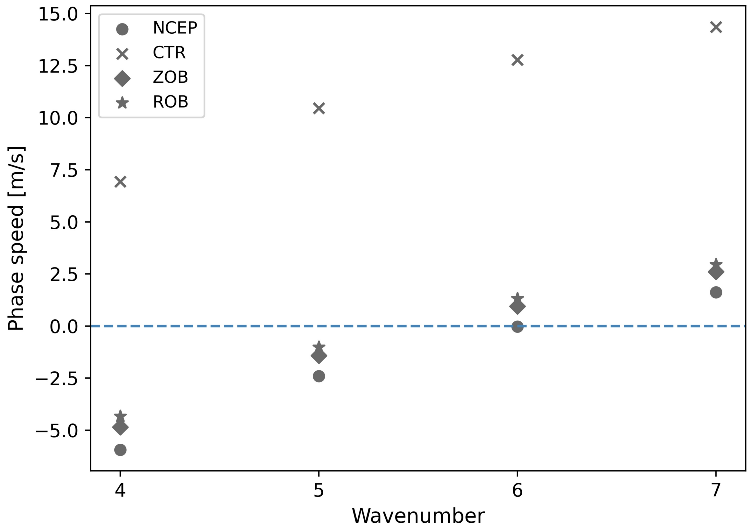

Figure 2. Phase speed for NCEP and the experiments in the Dry Core GCM. Calculated using the Rossby Wave dispersion relation (Eq. 7), considering the maximum barotropic averaged zonal wind in the northern mid-latitudes.

& Domeisen, 2022). However, the mere statistical difference of these five events found with our methodology concerning the event statistics from NCEP and the bias-corrected ones only confirms that an unrealistic basic state with respect to the boreal summer cannot provide a conducive environment for developing heatwave events that are statically consistent with observations.

We construct Hovmöller diagrams for streamfunction anomalies and the Rossby wave envelope for the bias-corrected experiments (Figure 3). In the ZOB and ROB, Rossby wave propagation along the midlatitudes even 15 days ahead of the events can be observed. It can be seen clearly how the individual troughs and ridges repeatedly amplify in almost the same longitudinal region, and the envelope shows the slow propagation of the packets with an overall timescale of 20-30 days. In contrast, all five events in the CTR are characterized by a much short timescale (3-7 days). Notice that when zonal variations are included in the experiment ROB, this Hovmöller result has more realistic features, and most importantly, the pattern is characterized by a wavenumber 5, which coincides with that associated with the occurrence of the events in a realistic atmosphere (Teng et al., 2013).

In addition, the latitudinal location of the jetstream changes for each experiment and it is known that the jetsetream serves as an efficient Rossby waveguide (Hoskins & Ambrizzi, 1993; Wirth et al., 2018), providing a preferred track for the Rossby Waves. The waveguide is shifted noticeably upward for the ZOB, while in the ROB, the latitudinal location closely resembles that observed in NCEP. As a consequence, the spatial location of the events is also more similar to that observed in the reanalysis.

3.3.1 A back-of-the-envelop calculation of the phase speeds

According to the linear wave theory, features of any wave can be derived from its dispersion relation, which is obtained considering the equation of motion, the assumptions of two-dimensional barotropic flow and some other simplifications described in (Vallis,

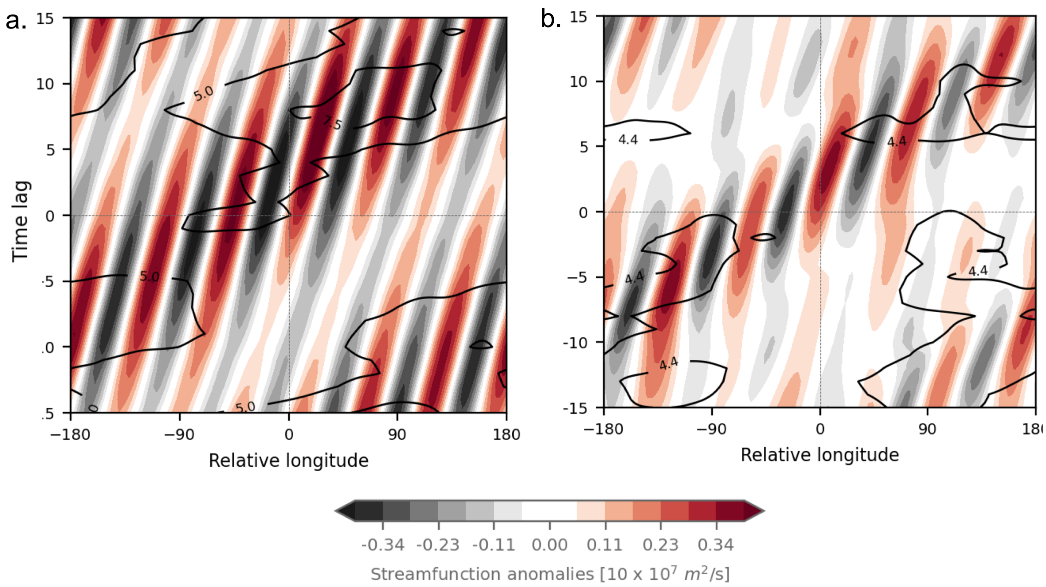

Figure 3. Hövmoller diagrams (longitude - time evolution) for streamfunction anomalies at 300 hPa between 30°N and 50°N with respect to all heatwaves detected (color shading) and Rossby Waves envelope (black contour) for the ZOB experiment (a.) and the ROB experiment (b.).

2017). Although these expression come from quite strong approximations, the solutions turn out to be relevant to the real atmosphere, and provide insight into the large-scale dynamics of mid-latitudes. The Rossby wave dispersion relation reads as follows:

$$\omega = Uk - \frac{\beta k}{k^2 + l^2} \tag{6}$$

Then, the phase speed of Rossby waves in the x direction follows:

$$c_p^x = \frac{\omega}{k} = U - \frac{\beta}{k^2 + l^2} \tag{7}$$

Where ω is the constant wave angular frequency in units of radians/time, β the Coriolis parameter in β - plane approximation, k^2+l^2 represent the square of the wavevector, where the wave numbers are given by $k = 2\pi/\lambda_x$, $l = 2\pi/\lambda_y$ with (λ_x, λ_y) the wavelengths in units of m. U is the density-weighted zonal-mean zonal-winds at the mid-latitudes in m/s, for which the density of the air in each layer is calculated considering the proportionality described in 8, where $z = -Hln(p/1000hPa)$.

$$\rho \propto e^{\frac{-z}{H}} \tag{8}$$

Since the phase speed relative to the background flow is always negative, these waves always propagate westward relative to the mean flow. When the phase lines are stationary relative to the ground, that is, $c_p^x = 0$ (Vallis, 2017), anomalous troughs lead to the occurrence and persistence of heat waves events.

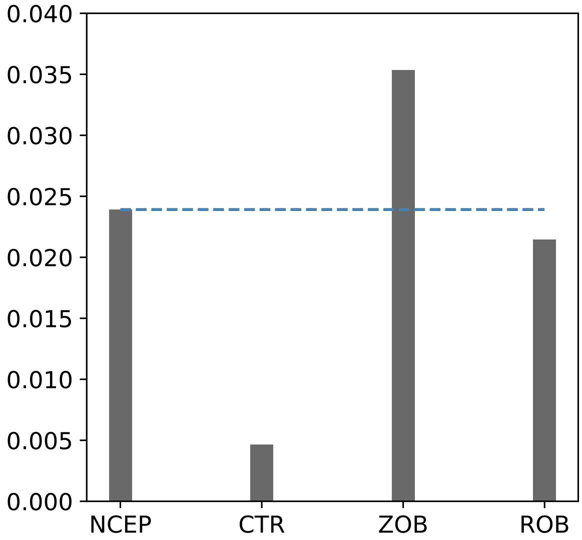

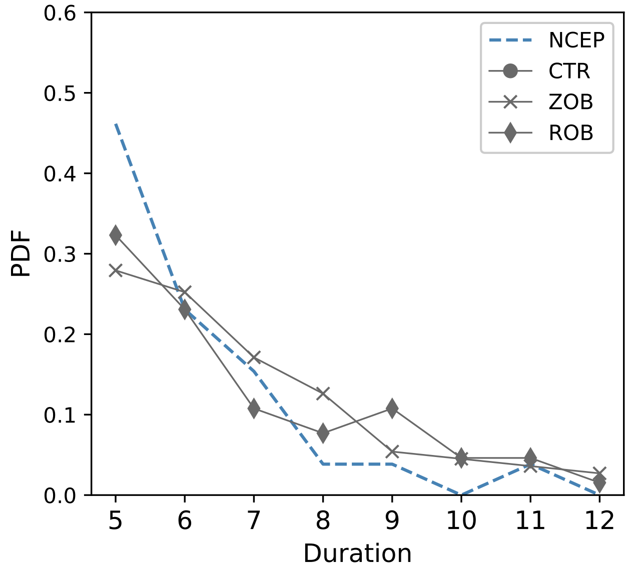

Figure 4. Comparison of statistics between NCEP and the experiments in the dry dynamical core GCM: Number of heatwaves waves over the total of analized days (upper) and the probability distribution function (PDF) of the duration of the events (bottom). For the CTR, the only 5 detected events correspond to a duration of 5 days.

4 Conclusions and discussions

The main objective of this study is to understand the role of the basic state on the propagation of Rossby Wave packets driving heat waves in the U.S. We use an idealized atmospheric model where physical parametrizations are substituted by a simple temperature relaxation. We implement the iterative procedure proposed by (Chang, 2006) to simulate the climatological atmosphere for the boreal summer (June, July, August). At the end, the model climate is forced to resemble the observed boreal summer mean flow structure without explicitly considering complicated physical processes (e.g., moisture, turbulence, clouds, etc.). This approach allows us to isolate the dry dynamics aspect of atmospheric circulation on heatwaves evolution, and the conclusions from the results can be summarized as follows:

- The climatological state drives the stationary Rossby wave propagation providing critical dynamical conditions for US heatwaves.
- A dry atmosphere with realistic boreal summer climatological state can produces a wavenumber-five Rossby Waves pattern, which often been seen in the observations preceding US heatwaves.

Previous studies show evidence of heat waves events preceded by a wavenumber five structure contained in Rossby Waves, and the link between the amplification of this pattern with its probability of heatwaves' occurrence. Our study helps to understand the origin of this pattern. It is demonstrated that a dynamical model resembling the actual zonal mean flow (ZOB) can clearly generate a similar Rossby Waves pattern, albeit characterized by zonal wavenumber six, preceding heat waves in the mid-latitudes. However, including the zonal asymmetries in the mean flow (ROB) is crucial for developing the specific wavenumber five structure, and consequently the statistics of the US heatwave events that are consistent with those in reanalysis.

The idealized model enables us to isolate exclusively on the dry atmospheric dynamics to understand the physical mechanism behind the interesting zonal wavenumber five pattern preceding frequent US heatwaves in the summer. While our idealized model contains only dry dynamics, the specific structure of climatological state must arise from the substantial contributions of various diabatic processes. On the one hand, local boundary conditions may play an important role on setting up a realistic climatological state. For example, (Donat et al., 2016; Lyon & Dole, 1995; McKinnon et al., 2016) show that the combination of local anomalous sea surface temperature (SST) patterns and atmospheric flow anomalies have contributed significantly to summer extremes. On the other hand, other studies also show the contribution of soil moisture conditions to heat waves by releasing surface diabatic heat (Seneviratne et al., 2010; Miralles et al., 2019) and even to the circumglobal circulation response of Rossby Waves (Douville & Chauvin, 2000; Douville, 2002; Koster et al., 2016). During summer, local land and oceanic conditions are important and may interact nonlinearly with atmospheric circulation states preceding heatwave events. Our next step is to study the dynamics under which local diabatic warming of soil moisture conditions impacts the amplitude of the wave number five pattern and its associated impacts on the statistics of the air temperature extremes in the US.

5 Open Research

The version of the Dry core GCM code used in this work is provided by the open-access data from Wu and Reichler (2018). We construted the target climatology for our simulations from the NCEP-NCAR Reanalysis 1 data provided by the NOAA PSL, Boulder, Colorado, USA. All the NCEP datasets used for this work can be accessed from $https://downloads.psl.noaa.gov/Datasets/ncep.reanalysis/Dailies/$. The temperature at all levels used to construct the inputs for the simulations, and also the velocity fields used for the comparison are in the folder called *pressure/* in that link, and the temperature at 2m in the folder *surface_gauss/*. The data also can be downloaded by following the FTP link in the section Source & References in the NCEP-NCAR Reanalysis 1 webpage: *https://psl.noaa.gov/data/gridded/data.ncep.reanalysis.html*.

The codes for this work and the final datasets obtained from the three simulations are located in the open-access repository *https://github.com/castanev/Dynamics_Heat_Waves.git* linked to Zenodo *DOI*: 10.5281/*zenodo*.7844138

Acknowledgments
The authors acknowledge to NOAA for providing NCEP-NCAR Reanalysis 1 data. They are also grateful to Zheng Wu and Thomas Reichler for providing openly the code of an updated version of the GFDL dry dynamical core GCM.

References

Chang, E. K. M. (2006, July). An Idealized Nonlinear Model of the Northern Hemisphere Winter Storm Tracks. *Journal of the Atmospheric Sciences*, *63*(7), 1818–1839. Retrieved 2023-03-24, from `https://journals.ametsoc.org/view/journals/atsc/63/7/jas3726.1.xml` (Publisher: American Meteorological Society Section: Journal of the Atmospheric Sciences) doi: 10.1175/JAS3726.1

Chen, P., & Newman, M. (1998, October). Rossby Wave Propagation and the Rapid Development of Upper-Level Anomalous Anticyclones during the 1988 U.S. Drought. *Journal of Climate*, *11*(10), 2491–2504. Retrieved 2023-04-07, from `https://journals.ametsoc.org/view/journals/clim/11/10/1520-0442_1998_011_2491_rwpatr_2.0.co_2.xml` (Publisher: American Meteorological Society Section: Journal of Climate) doi: 10.1175/1520-0442(1998)011⟨2491:RWPATR⟩2.0.CO;2

Ding, Q., & Wang, B. (2005, September). Circumglobal Teleconnection in the Northern Hemisphere Summer. *Journal of Climate*, *18*(17), 3483–3505. Retrieved 2023-04-07, from `https://journals.ametsoc.org/view/journals/clim/18/17/jcli3473.1.xml` (Publisher: American Meteorological Society Section: Journal of Climate) doi: 10.1175/JCLI3473.1

Donat, M. G., King, A. D., Overpeck, J. T., Alexander, L. V., Durre, I., & Karoly, D. J. (2016, January). Extraordinary heat during the 1930s US Dust Bowl and associated large-scale conditions. *Climate Dynamics*, *46*(1), 413–426. Retrieved 2023-04-07, from `https://doi.org/10.1007/s00382-015-2590-5` doi: 10.1007/s00382-015-2590-5

Douville, H. (2002, April). Influence of Soil Moisture on the Asian and African Monsoons. Part II: Interannual Variability. *Journal of Climate*, *15*(7), 701–720. Retrieved 2023-04-07, from `https://journals.ametsoc.org/view/journals/clim/15/7/1520-0442_2002_015_0701_iosmot_2.0.co_2.xml` (Publisher: American Meteorological Society Section: Journal of Climate) doi: 10.1175/1520-0442(2002)015⟨0701:IOSMOT⟩2.0.CO;2

Douville, H., & Chauvin, F. (2000, October). Relevance of soil moisture for seasonal climate predictions: a preliminary study. *Climate Dynamics*, *16*(10), 719–736. Retrieved 2023-04-07, from `https://doi.org/10.1007/s003820000080` doi: 10.1007/s003820000080

Feldstein, S. B. (2000, December). The Timescale, Power Spectra, and Climate Noise Properties of Teleconnection Patterns. *Journal of Climate*, *13*(24), 4430–4440. Retrieved 2023-03-31, from `https://journals.ametsoc.org/view/journals/clim/13/24/1520-0442_2000_013_4430_ttpsac_2.0.co_2.xml` (Publisher: American Meteorological Society Section: Journal of Climate) doi: 10.1175/1520-0442(2000)013⟨4430:TTPSAC⟩2.0.CO;2

Fragkoulidis, G., & Wirth, V. (2020, October). Local Rossby Wave Packet Amplitude, Phase Speed, and Group Velocity: Seasonal Variability and Their Role in Temperature Extremes. *Journal of Climate*, *33*(20), 8767–8787. Retrieved 2023-04-07, from https://journals.ametsoc.org/view/journals/clim/33/20/jcliD190377.xml (Publisher: American Meteorological Society Section: Journal of Climate) doi: 10.1175/JCLI-D-19-0377.1

Held, I. M. (2005, November). The Gap between Simulation and Understanding in Climate Modeling. *Bulletin of the American Meteorological Society*, *86*(11), 1609–1614. Retrieved 2023-04-15, from https://journals.ametsoc.org/view/journals/bams/86/11/bams-86-11-1609.xml (Publisher: American Meteorological Society Section: Bulletin of the American Meteorological Society) doi: 10.1175/BAMS-86-11-1609

Held, I. M., & Suarez, M. J. (1994, October). A Proposal for the Intercomparison of the Dynamical Cores of Atmospheric General Circulation Models. *Bulletin of the American Meteorological Society*, *75*(10), 1825–1830. Retrieved 2023-03-24, from https://journals.ametsoc.org/view/journals/bams/75/10/1520-0477_1994_075_1825_apftio_2_0_co_2.xml (Publisher: American Meteorological Society Section: Bulletin of the American Meteorological Society) doi: 10.1175/1520-0477(1994)075⟨1825:APFTIO⟩2.0.CO;2

Hoskins, B. J., & Ambrizzi, T. (1993, June). Rossby Wave Propagation on a Realistic Longitudinally Varying Flow. *Journal of the Atmospheric Sciences*, *50*(12), 1661–1671. Retrieved 2023-04-07, from https://journals.ametsoc.org/view/journals/atsc/50/12/1520-0469_1993_050_1661_rwpoar_2_0_co_2.xml (Publisher: American Meteorological Society Section: Journal of the Atmospheric Sciences) doi: 10.1175/1520-0469(1993)050⟨1661:RWPOAR⟩2.0.CO;2

Jiménez-Esteve, B., & Domeisen, D. I. (2022, July). The role of atmospheric dynamics and large-scale topography in driving heatwaves. *Quarterly Journal of the Royal Meteorological Society*, *148*(746), 2344–2367. Retrieved 2023-04-07, from https://onlinelibrary.wiley.com/doi/10.1002/qj.4306 doi: 10.1002/qj.4306

Koster, R. D., Chang, Y., Wang, H., & Schubert, S. D. (2016, October). Impacts of Local Soil Moisture Anomalies on the Atmospheric Circulation and on Remote Surface Meteorological Fields during Boreal Summer: A Comprehensive Analysis over North America. *Journal of Climate*, *29*(20), 7345–7364. Retrieved 2023-04-07, from https://journals.ametsoc.org/view/journals/clim/29/20/jcli-d-16-0192.1.xml (Publisher: American Meteorological Society Section: Journal of Climate) doi: 10.1175/JCLI-D-16-0192.1

Lyon, B., & Dole, R. M. (1995, June). A Diagnostic Comparison of the 1980 and 1988 U.S. Summer Heat Wave-Droughts. *Journal of Climate*, *8*(6), 1658–1675. Retrieved 2023-04-07, from https://journals.ametsoc.org/view/journals/clim/8/6/1520-0442_1995_008_1658_adcota_2_0_co_2.xml (Publisher: American Meteorological Society Section: Journal of Climate) doi: 10.1175/1520-0442(1995)008⟨1658:ADCOTA⟩2.0.CO;2

McKinnon, K. A., Rhines, A., Tingley, M. P., & Huybers, P. (2016, May). Long-lead predictions of eastern United States hot days from Pacific sea surface temperatures. *Nature Geoscience*, *9*(5), 389–394. Retrieved 2023-04-07, from https://www.nature.com/articles/ngeo2687 (Number: 5 Publisher: Nature Publishing Group) doi: 10.1038/ngeo2687

Meehl, G. A., & Tebaldi, C. (2004, August). More Intense, More Frequent, and Longer Lasting Heat Waves in the 21st Century. *Science*, *305*(5686), 994–997. Retrieved 2023-04-07, from https://www.science.org/doi/10.1126/science.1098704 (Publisher: American Association for the Advancement of Science) doi: 10.1126/science.1098704

Miralles, D. G., Gentine, P., Seneviratne, S. I., & Teuling, A. J. (2019, January). Land–atmospheric feedbacks during droughts and heatwaves: state of the science and current challenges. *Annals of the New York Academy of Sciences*, *1436*(1), 19–35. Retrieved 2023-04-07, from https://www.ncbi.nlm.nih.gov/pmc/articles/PMC6378599/ doi: 10.1111/nyas.13912

Pedlosky, J. (2003). *Waves in the Ocean and Atmosphere: Introduction to Wave Dynamics* (2003rd edition ed.). Berlin ; New York: Springer.

Röthlisberger, M., Frossard, L., Bosart, L. F., Keyser, D., & Martius, O. (2019, June). Recurrent Synoptic-Scale Rossby Wave Patterns and Their Effect on the Persistence of Cold and Hot Spells. *Journal of Climate*, *32*(11), 3207–3226. Retrieved 2023-04-07, from https://journals.ametsoc.org/view/journals/clim/32/11/jcli-d-18-0664.1.xml doi: 10.1175/JCLI-D-18-0664.1

Schubert, S., Wang, H., & Suarez, M. (2011, September). Warm Season Subseasonal Variability and Climate Extremes in the Northern Hemisphere: The Role of Stationary Rossby Waves. *Journal of Climate*, *24*(18), 4773–4792. Retrieved 2023-04-15, from https://journals.ametsoc.org/view/journals/clim/24/18/jcli-d-10-05035.1.xml (Publisher: American Meteorological Society Section: Journal of Climate) doi: 10.1175/JCLI-D-10-05035.1

Seneviratne, S. I., Corti, T., Davin, E. L., Hirschi, M., Jaeger, E. B., Lehner, I., ... Teuling, A. J. (2010, May). Investigating soil moisture–climate interactions in a changing climate: A review. *Earth-Science Reviews*, *99*(3), 125–161. Retrieved 2023-04-15, from https://www.sciencedirect.com/science/article/pii/S0012825210000139 doi: 10.1016/j.earscirev.2010.02.004

Teng, H., Branstator, G., Wang, H., Meehl, G. A., & Washington, W. M. (2013, December). Probability of US heat waves affected by a subseasonal planetary wave pattern. *Nature Geoscience*, *6*(12), 1056–1061. Retrieved 2023-03-24, from https://www.nature.com/articles/ngeo1988 (Number: 12 Publisher: Nature Publishing Group) doi: 10.1038/ngeo1988

Vallis, G. K. (2017). *Atmospheric and Oceanic Fluid Dynamics: Fundamentals and Large-Scale Circulation* (2nd ed.). Cambridge: Cambridge University Press. Retrieved 2023-03-01, from https://www.cambridge.org/core/books/atmospheric-and-oceanic-fluid-dynamics/41379BDDC4257CBE11143C466F6428A4 doi: 10.1017/9781107588417

Wirth, V., Riemer, M., Chang, E. K. M., & Martius, O. (2018, July). Rossby Wave Packets on the Midlatitude Waveguide—A Review. *Monthly Weather Review*, *146*(7), 1965–2001. Retrieved 2023-04-05, from https://journals.ametsoc.org/view/journals/mwre/146/7/mwr-d-16-0483.1.xml (Publisher: American Meteorological Society Section: Monthly Weather Review) doi: 10.1175/MWR-D-16-0483.1

Wu, Z., & Reichler, T. (2018). Towards a more earth-like circulation in idealized models. Retrieved from https://doi.org/ doi: 10.1029/2018MS001356

Zimin, A. V., Szunyogh, I., Patil, D. J., Hunt, B. R., & Ott, E. (2003, May). Extracting Envelopes of Rossby Wave Packets. *Monthly Weather Review*, *131*(5), 1011–1017. Retrieved 2023-03-24, from https://journals.ametsoc.org/view/journals/mwre/131/5/1520-0493_2003_131_1011_eeorwp_2.0.co_2.xml (Publisher: American Meteorological Society Section: Monthly Weather Review) doi: 10.1175/1520-0493(2003)131⟨1011:EEORWP⟩2.0.CO;2

The Role of Climatological State on Driving US Heat Waves Through Rossby Waves Packets

Valentina Castañeda[1], **Lei Wang**[1]

[1]Department of Earth, Atmospheric, and Planetary Sciences, Purdue University

Key Points:

- The climatological state drives the stationary Rossby wave propagation providing critical dynamical conditions for heat waves in the US.
- A dry atmospheric model with a corrected climatological state generates heatwaves that are statistically consistent with observations.
- The slowly propagating Rossby wave packets with a timescale of 20-30 days can be a source of intraseasonal predictability.

Corresponding author: Lei Wang, `leiwang@purdue.edu`

Abstract

While heat waves are local extreme weather events, a planetary Rossby wave pattern is statistically related to the occurrence of heat waves events in the U.S. However, whether such planetary wave patterns cause the enhanced statistics of local heat waves or as a coincidence is debatable. In this work, we hypothesize that the atmospheric climatological state dictates the slowly propagating wave pattern, which sets up a conducive large-scale environment for local US heat waves. We implement an idealized dry dynamic core model with an iterative approach to simulate the realistic North American summer climatological state. As the model can generate similar large-scale planetary wave patterns propagating throughout North America, significantly more heatwaves are generated, and the statistics of heat waves become consistent with that estimated in reanalysis products. The slowly propagating Rossby wave packets with a timescale of 20-30 days can serve as a new source of intraseasonal predictability.

Plain Language Summary

Heatwaves are the leading weather-related killer in the United States and affect mainly the most vulnerable communities. These extreme events are statistically related to a large-scale wave pattern of Rossby waves that features a zonal wavenumber five structure. To find out what controls this wave pattern, we use a simple general circulation model that only contains dry dynamics without complicated interactions with moisture or clouds. We found that by modifying the climatological state of temperature and velocity fields based on the observed structure from the Northern Hemisphere summer, we can observe the same wave number five pattern developing days before the heatwave events, resembling that from the observations. This result suggests that the climatological state of the Northern Hemispheric summer provides a conducive environment for heatwaves in the U.S. due to the slowed-down propagation speed of the Rossby wave packets. A deeper understanding of its dynamics is crucial because, as this pattern develops up to 20 days ahead of the extremes, the underlying physical process governing this pattern may serve as a source of predictability on the Subseasonal-to-Seasonal (S2S) timescale, a current gap of forecasts between weather and climate.

1 Introduction

Over the coming century, climate change is expected to increase average summer temperatures and the severity of extreme heat linked with heat waves events. In the United States, the frequency, intensity, and duration of heat waves have been increasing rapidly in recent decades, and this behavior is projected to continue in the next decades (Meehl & Tebaldi, 2004). Currently, forecasters in the United States can only predict extreme events up to 10 days in advance because, unlike in the tropics, circulation in the mid-latitudes is more chaotic as it is dominated by climatic noise (Feldstein, 2000).

However, it is intriguing to hypothesize that certain atmospheric circulation states can be substantially more predictable than the average scenario, because these circulation regimes are associated with low-frequency patterns (Schubert et al., 2011). With this in mind, and considering that different studies have suggested that propagating stationary Rossby Waves play an important role in the mid-latitude atmospheric variability, the scientific community recently has increased interest in the connection between extreme weather events and large-scale atmospheric patterns such as Rossby Wave Packets (Chen & Newman, 1998; Schubert et al., 2011; Fragkoulidis & Wirth, 2020).

In many of the investigated cases, the extreme weather was linked to an upper-tropospheric trough (i.e., a breaking Rossby Waves). For example, Chen and Newman (1998) suggests that Rossby Waves originating in the west Pacific were the key in initiating intense anomalous anticyclones during the 1988 U.S. drought. Also, Schubert et al. (2011) relates this large-scale pattern with monthly mean precipitation and surface temperature variability over many regions of the extratropical land areas, including the northern U.S., parts of Canada, Europe, and Russia. Following the same approach, Ding and Wang (2005) found an interannually varying Northern Hemisphere circumglobal pattern with a preferred wavenumber five structure. This particular structure is confined within the waveguide associated with the summer north jet stream in the stationary state and is linked to significant surface air temperature and rainfall anomalies in western Europe, European Russia, India, East Asia, and North America. In a more recent study Teng et al. (2013), more concrete evidence has been shown of the relationship between the occurrence of heatwaves in the U.S. and the same wavenumber five pattern developing as early as 20 days ahead of the events. Despite the growing evidence for the concurrences of this interesting wave number five pattern, the physical mechanism that drives the atmospheric pattern and thus determines heatwaves has yet to be understood.

This study aims to understand better the fundamental role of atmospheric dynamics in the evolution of U.S. heat waves based on the hypothesis that the climatological state for the Northern Hemisphere summer drives the stationary Rossby wave propagation providing critical dynamical conditions for heat waves in the U.S. Inspired by the motivation to look for the simplest possible model in the climate model hierarchies (Held, 2005), we adopt an idealized dry dynamical core that allows for a bias correction of the mean flow structure without physical parameterizations. This approach allows us to isolate the role of intrinsic planetary waves in the evolution of extreme events.

2 Data and Methods

2.1 Reanalysis products

For the observational analysis, the NCEP/NCAR reanalysis of the National Oceanic and Atmospheric Administration (NOAA) was implemented. The surface air temperature (SAT), all levels of temperature and the meridional and zonal components of the wind at 300 hPa (V_{300} and U_{300}) were obtained from these databases with a spatial resolution of 2.5° and daily temporal resolution from 1948 to 2023.

2.2 An Idealized GCM with realistic climatological basic state

Idealized general circulation models are commonly used for the study of atmospheric dynamics. A dry dynamical core model solves the primitive equations on the sphere by nudging the climatological temperature field toward a prescribed structure of radiative equilibrium temperature (T_{eq}). Essentially, this process isolates the dry atmospheric dynamics from the complex physical parameterizations.

We use the open-access updated version from (Wu & Reichler, 2018) of the spectral dynamical core model proposed by (Held & Suarez, 1994) for the Geophysical Fluid Dynamics Laboratory (GFDL). The model has a horizontal resolution of T42 (64x128 grid) and 40 vertical σ levels between the surface and 0.01 hPa. To represent the boundary-layer friction, Rayleigh drag is used to remove momentum in the lower troposphere between the surface and $\sigma = 0.7$. By default configurations of this model, the temperature is forced by Newtonian relaxation toward a prescribed equilibrium temperature as follows:

$$\frac{\partial T}{\partial t} = \frac{T - T_{eq}}{\tau} \tag{1}$$

where τ is the prescribed relaxation timescale.

Since the primary purpose of this study is to examine how the atmospheric basic state controls the large-scale Rossby Wave pattern with a zonal wavenumber five struc-

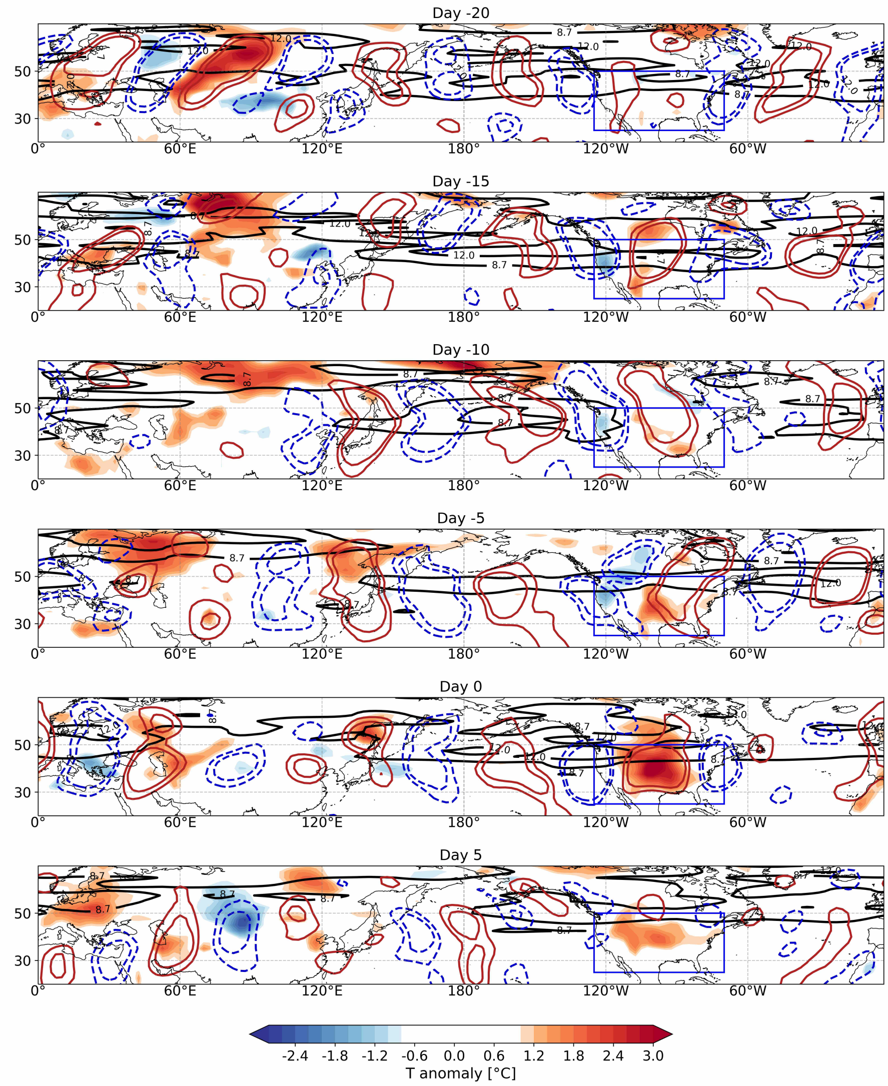

Figure 1. **Evolution of heat waves 20 days ahead of the events**: Red and dashed blue contours represent composites of 200hPa streamfunction anomalies at ± 0.05, 0.08 (red as positives). Shading represents surface air temperature anomaly and black contours represent the Rossby Wave Packet envelope at levels 8.7, 12 m/s.

ture driving local heat waves in the US, the model includes the iterative procedure proposed by Chang (2006) to simulate the climatological basic state of the atmosphere in the idealized model. This consists of iterating the radiative equilibrium temperature profile so that at the end of the iterations, the model climate closely resembles the desired target climate (see Supporting Information for more details of the methodology). The iteration uses a fixed equilibrium temperature for each N step (T_{eq}) in a run of 62 years, for a total of 21630 days after eliminating the first 1000 days of simulation. Then, we calculate the model simulated temperature climatology $T_{(N)}$ and correct it concerning basic state from the NCEP reanalysis data T_R. The next iteration step N+1 is calculated according to:

$$T_{eq(N+1)} = T_{eq(N)} - \frac{2}{3}(T_{(N)} - T_R), N = 1, 2, 3... \quad (2)$$

To assess the role of the climatological basic state, we carry out three experiments as follows:

- **Held and Suarez 1994 configuration (CTR)**: the zonal-mean temperature structure is relaxed toward a prescribed equinoctial radiative-equilibrium state. It's the default configuration described in detail in (Held & Suarez, 1994) and leads to a climatological state close to the observed annual mean climatological state.
- **Zonally-symmetric boreal summer (ZOB)**: The ratiative forcing T_R described in section 2.2 and in eq. 2 is set by the two-dimensional (i.e., latitude-pressure) basic state from the NCEP reanalysis data. For this experiment, we use the zonally symmetrical distribution of temperature for the climatological boreal summer (June, July, and August) between 1948 and 2021.
- **Realistic Northern Hemisphere summer (ROB)**: The full three-dimensional structure of the radiative forcing T_R is obtained from the climatological boreal summer from NCEP, especially including zonal asymmetries. This bias correction includes zonal variations in T_{eq}, which can be related to zonal variations in diabatic heating as discussed in Chang (2006) work.

2.3 Heat waves identification

A heatwave event is set as at least five consecutive days with more than around 900000 km^2 over the US continental area (125W – 70W, 25N – 50N) with daily averaged SAT exceeding a threshold value, and the center of these warm points, considered as the point of maximum temperature, does not move faster than 5 latitude or longitude per day. The temperature threshold varies spatially as well as with the day of the year. It was established as the percentile 97.5 of the historical SAT. This approach follows Teng et al. (2013).

2.4 Rossby Wave Packets evolution

As this study aims to understand the dynamics behind heat waves, it is necessary to look at the evolution of the Rossby Waves Packets driving extreme events from observational data and modeling outputs. Both the eddy phase speeds and their group velocity are important physical properties of Rossby Wave Packets' propagation. In particular, the eddy phase speed indicates the propagation speed of individual troughs within Rossby Waves Packets. It can thus be critical for the persistence of extreme surface weather (Röthlisberger et al., 2019). On the other hand, the group velocity reflects how quickly the whole packet propagates locally and represents the rate at which the Rossby waves transfer energy horizontally (Pedlosky, 2003). Based on the Rossby Waves Packets' progression in longitude and time, we compute the envelope of the meridional wind indicating their preferred regions of formation and decay. Specifically, we estimate the Rossby

Waves Packets' propagation by constructing Hovmöller diagrams using streamfunction anomalies at 300 hPa and the corresponding Rossby Waves Packets' envelope.

Subsequently, we calculate the local (in space and time) group velocity using the Rossby Waves Packets' envelope, which reflects how the flow features of enhanced meridional wind amplitude propagate in the zonal and meridional directions (Fragkoulidis & Wirth, 2020). We implemented the method proposed by Zimin et al. (2003) for the calculation of Rossby Waves Packets' envelope involving the Hilbert transform along circles of constant latitude combined with a restriction of the zonal wavenumber to a specified interval, which in this case corresponds to wavenumbers between 3 and 11. We implement this methodology using the meridional wind, which is usually implemented for the diagnosis of meridional deviations from the zonal flow, and is particularly well suited for the detection of Rossby waves. Specifically, we take the upper-tropospheric (300 hPa) meridional wind which features strong Rossby Waves Packet's activities (Wirth et al., 2018). The meridional wind anomaly $v(x)$ is considered on an equidistant grid along a latitude circle, where $x = 2\pi/N$ with $0 < x \leq 2\pi$, N is an even integer, and $l = 1, 2, ..., N$. The Fourier transform of the real function $v(x)$ is computed as:

$$\hat{v}_k = \frac{1}{N} \sum_{l=1}^{N} v\left(\frac{2\pi l}{N}\right) e^{-2\pi ik/N}, \left(K = -\frac{N}{2} + 1, ..., \frac{N}{2}\right) \tag{3}$$

The inverse Fourier transform is applied to a selected band of the positive wavenumber half of the Fourier spectrum:

$$w\left(\frac{2\pi l}{N}\right) = 2 \sum_{k=k_{min}}^{k_{max}} \hat{v}_k e^{2\pi ik/N} \tag{4}$$

Finally, the packet envelope is calculated as follows:

$$A(2\pi l/N) = |w(2\pi l/N)| \tag{5}$$

3 Results

3.1 Stationary waves preceding heat waves in reanalysis

From the reanalysis data, we found 165 heat waves days from 26 events found in the 75 summers from NCEP. We look at the temporal evolution of the planetary waves preceding the events by constructing composites from day -20 to day 5 (Figure 1), where we designate the first day of a heatwave as day 0. We used daily sub-seasonal anomalies at 300 hPa streamfunction calculated as the daily departures from the long-term mean and from the seasonal (June-July-August) mean of the particular year. These anomalies were spatially filtered, considering only wavelengths between 2800 km and 10000 km to consider only the wavenumbers of interest and avoid noise. Defined low and high-pressure centers can be seen moving slowly westward, expected behavior for Rossby Wave propagation in the days leading up to the extreme event. Although several of the troughs and ridges are clearly seen, it cannot be readily determined whether the wavenumber is 5 or 6. This difficulty may be explained by the scarcity of the events in the reanalysis, which are rare by definition. On the other hand, the Rossby Waves amplitudes shown by the envelope reflect the energy transport by the propagating waves. Notably, the large amplitudes of the envelope are seen in the two ocean basins, consistent with the zones where the Rossby Waves tend to reach large amplitudes and phase speeds. (Fragkoulidis & Wirth, 2020).

3.2 Climatology on the idealized simulations

We first discuss the climatological circulation characteristics obtained for the 21630 analyzed days in each experiment (See Supporting Information Figures S1. and S2). As we used a prescribed temperature from NCEP reanalysis data for the Newtonian relaxation in the model, the bias-corrected experiments resemble the zonally symmetric and asymmetric Northern Hemispheric summer in the real atmosphere by construction. It means the temporal mean of the spatial distribution of the temperature, the barotropic averaged zonal wind, and the vertical distribution of the zonal wind, in general, resemble the atmosphere. It should be clarified that although some features of the corrected climatological state are not realistic, especially in the vertical distribution, they are realistic for the key latitudes of interest in this work (between 30°N and 60°N). Note that the basic atmospheric state of the CTR differs spatially and in magnitude from the real atmosphere. While in the real atmosphere, the peak jet intensity is about 10 m/s during the winter, the CTR exhibits a peak of more than 20 m/s. This is because the T_{eq} in the initial configuration is set based on annual climatology values rather than summer seasonality.

The expected phase speeds corresponding to the climatological zonal winds are calculated for different wavenumbers and compared to the results from reanalysis for the boreal summer (Figure 2). This is to elucidate the expected stationarity for the wave tracks preceding the events. The wavenumbers 5 and 6 have phase speeds close to zero for both observations and the bias-corrected experiments ZOB and ROB. From this calculation, we expect that any pattern associated with any of these wavenumbers can be developed before the events in the corrected experiments. However, the wavenumber five tends to precede U.S. heat waves (Teng et al., 2013). Although in this result for NCEP, it is wave number 6 that has phase velocity closest to 0, it should be noted that although the Rossby wave dispersion relation delves into the large-scale dynamics of mid-latitudes, it is based on a linearized approximation of the equations of motion, and may not accurately represent the behavior of atmospheric waves in situations where nonlinear interactions and other complicating factors are important. On the other hand, the overly strong eddy phase speed obtained for the CTR run again reflect the unrealistic climatology compared to the boreal summer, which provides a non-favorable large-scale environment for developing surface heatwaves. This explains the scarcity of heatwaves in the CTR.

3.3 Heat Waves driven by Intrinsic Planetary Wave pattern

Now that the model resembles the atmospheric basic state for the boreal summer, we can test our hypothesis that the basic state drives the stationary Rossby Waves propagation hence determining heat waves in the mid-latitudes. We must answer, firstly, if it resembles the actual statistics of heat waves, and secondly, if it resembles the atmospheric pattern preceding the events.

We compared the probability of heat waves days and the probability distribution function (PDF) of the events between the experiments and NCEP (Figure 4). We found 111 events and 765 heat waves days in the bias-corrected symmetrical case and 65 and 464 heat waves days in the asymmetric one. Both bias-corrected experiments resemble the PDF of the duration of the events in the reanalysis. However, only the one considering asymmetries (ROB) has a probability of occurrence of heat waves days similar to that found in the reanalysis. In contrast, the overly strong jetstream in the CTR run experiment can explain the extremely rare of similar heatwaves (only 5 events); the phase speeds of troughs are too high to drive persistent weather conditions. Indeed, by changing the detection methodology for this experiment, we can find slightly more events in the CTR. For example, considering a lower velocity of the center of the warm points or a minimum duration of the events shorter than five days, as shown in (Jiménez-Esteve

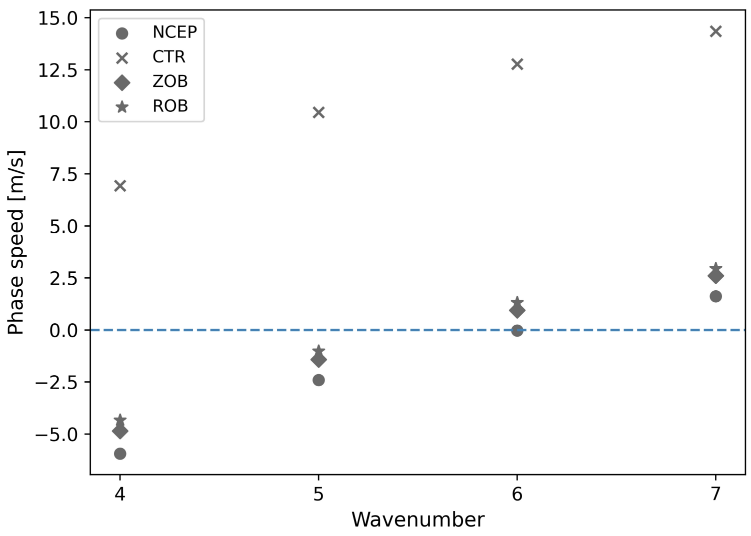

Figure 2. Phase speed for NCEP and the experiments in the Dry Core GCM. Calculated using the Rossby Wave dispersion relation (Eq. 7), considering the maximum barotropic averaged zonal wind in the northern mid-latitudes.

& Domeisen, 2022). However, the mere statistical difference of these five events found with our methodology concerning the event statistics from NCEP and the bias-corrected ones only confirms that an unrealistic basic state with respect to the boreal summer cannot provide a conducive environment for developing heatwave events that are statically consistent with observations.

We construct Hovmöller diagrams for streamfunction anomalies and the Rossby wave envelope for the bias-corrected experiments (Figure 3). In the ZOB and ROB, Rossby wave propagation along the midlatitudes even 15 days ahead of the events can be observed. It can be seen clearly how the individual troughs and ridges repeatedly amplify in almost the same longitudinal region, and the envelope shows the slow propagation of the packets with an overall timescale of 20-30 days. In contrast, all five events in the CTR are characterized by a much short timescale (3-7 days). Notice that when zonal variations are included in the experiment ROB, this Hovmöller result has more realistic features, and most importantly, the pattern is characterized by a wavenumber 5, which coincides with that associated with the occurrence of the events in a realistic atmosphere (Teng et al., 2013).

In addition, the latitudinal location of the jetstream changes for each experiment and it is known that the jetsetream serves as an efficient Rossby waveguide (Hoskins & Ambrizzi, 1993; Wirth et al., 2018), providing a preferred track for the Rossby Waves. The waveguide is shifted noticeably upward for the ZOB, while in the ROB, the latitudinal location closely resembles that observed in NCEP. As a consequence, the spatial location of the events is also more similar to that observed in the reanalysis.

3.3.1 A back-of-the-envelop calculation of the phase speeds

According to the linear wave theory, features of any wave can be derived from its dispersion relation, which is obtained considering the equation of motion, the assumptions of two-dimensional barotropic flow and some other simplifications described in (Vallis,

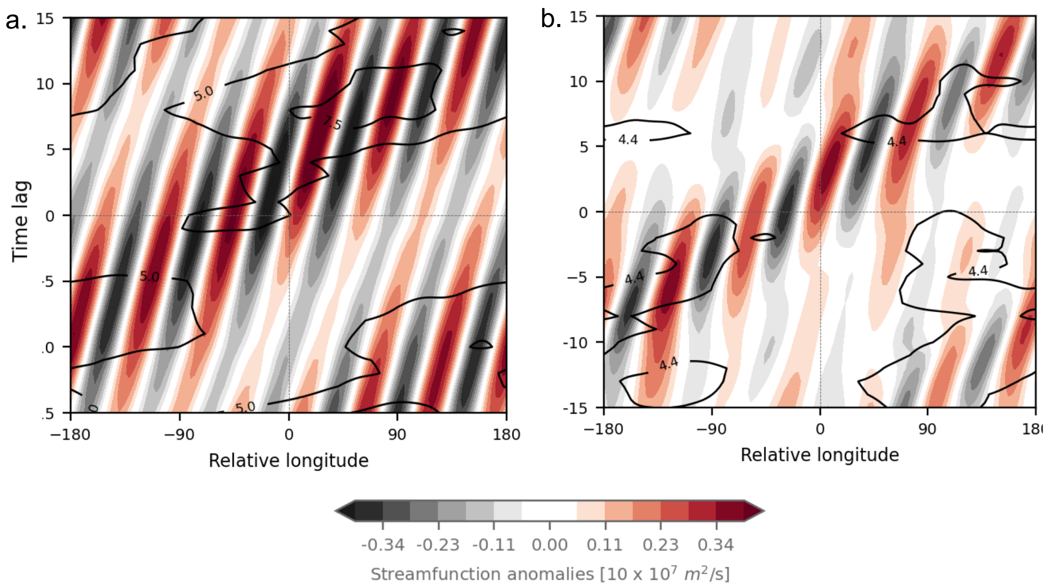

Figure 3. Hövmoller diagrams (longitude - time evolution) for streamfunction anomalies at 300 hPa between 30°N and 50°N with respect to all heatwaves detected (color shading) and Rossby Waves envelope (black contour) for the ZOB experiment (a.) and the ROB experiment (b.).

2017). Although these expression come from quite strong approximations, the solutions turn out to be relevant to the real atmosphere, and provide insight into the large-scale dynamics of mid-latitudes. The Rossby wave dispersion relation reads as follows:

$$\omega = Uk - \frac{\beta k}{k^2 + l^2} \tag{6}$$

Then, the phase speed of Rossby waves in the x direction follows:

$$c_p^x = \frac{\omega}{k} = U - \frac{\beta}{k^2 + l^2} \tag{7}$$

Where ω is the constant wave angular frequency in units of radians/time, β the Coriolis parameter in β - plane approximation, k^2+l^2 represent the square of the wavevector, where the wave numbers are given by $k = 2\pi/\lambda_x$, $l = 2\pi/\lambda_y$ with (λ_x, λ_y) the wavelengths in units of m. U is the density-weighted zonal-mean zonal-winds at the mid-latitudes in m/s, for which the density of the air in each layer is calculated considering the proportionality described in 8, where $z = -Hln(p/1000hPa)$.

$$\rho \propto e^{\frac{-z}{H}} \tag{8}$$

Since the phase speed relative to the background flow is always negative, these waves always propagate westward relative to the mean flow. When the phase lines are stationary relative to the ground, that is, $c_p^x = 0$ (Vallis, 2017), anomalous troughs lead to the occurrence and persistence of heat waves events.

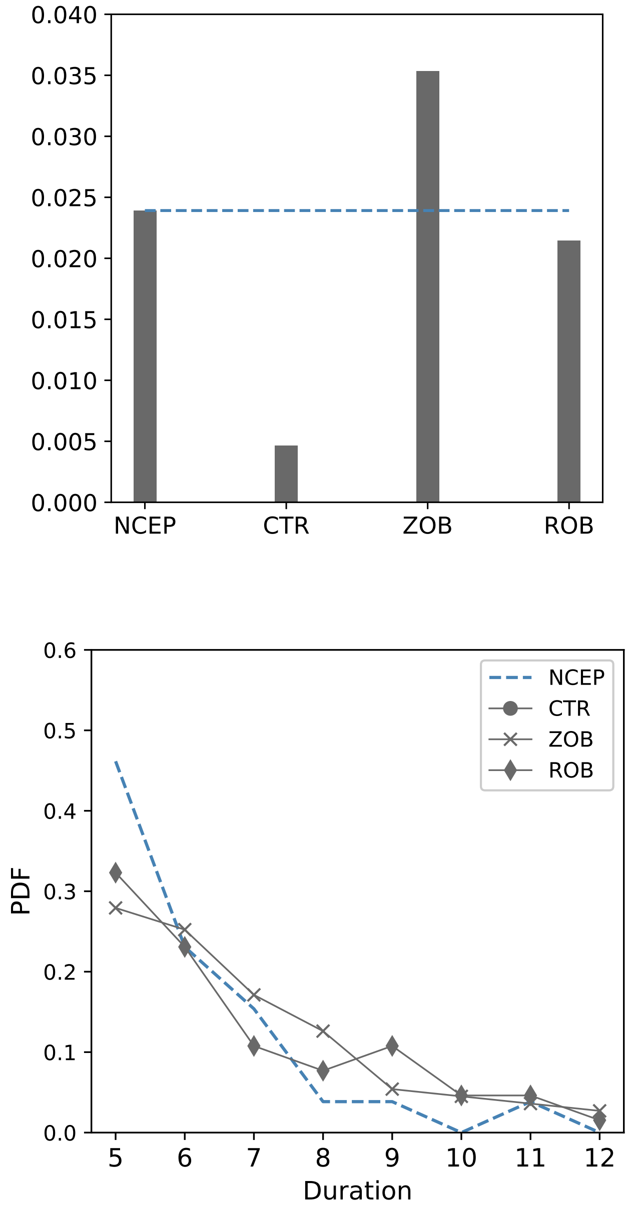

Figure 4. Comparison of statistics between NCEP and the experiments in the dry dynamical core GCM: Number of heatwaves waves over the total of analized days (upper) and the probability distribution function (PDF) of the duration of the events (bottom). For the CTR, the only 5 detected events correspond to a duration of 5 days.

4 Conclusions and discussions

The main objective of this study is to understand the role of the basic state on the propagation of Rossby Wave packets driving heat waves in the U.S. We use an idealized atmospheric model where physical parametrizations are substituted by a simple temperature relaxation. We implement the iterative procedure proposed by (Chang, 2006) to simulate the climatological atmosphere for the boreal summer (June, July, August). At the end, the model climate is forced to resemble the observed boreal summer mean flow structure without explicitly considering complicated physical processes (e.g., moisture, turbulence, clouds, etc.). This approach allows us to isolate the dry dynamics aspect of atmospheric circulation on heatwaves evolution, and the conclusions from the results can be summarized as follows:

- The climatological state drives the stationary Rossby wave propagation providing critical dynamical conditions for US heatwaves.
- A dry atmosphere with realistic boreal summer climatological state can produces a wavenumber-five Rossby Waves pattern, which often been seen in the observations preceding US heatwaves.

Previous studies show evidence of heat waves events preceded by a wavenumber five structure contained in Rossby Waves, and the link between the amplification of this pattern with its probability of heatwaves' occurrence. Our study helps to understand the origin of this pattern. It is demonstrated that a dynamical model resembling the actual zonal mean flow (ZOB) can clearly generate a similar Rossby Waves pattern, albeit characterized by zonal wavenumber six, preceding heat waves in the mid-latitudes. However, including the zonal asymmetries in the mean flow (ROB) is crucial for developing the specific wavenumber five structure, and consequently the statistics of the US heatwave events that are consistent with those in reanalysis.

The idealized model enables us to isolate exclusively on the dry atmospheric dynamics to understand the physical mechanism behind the interesting zonal wavenumber five pattern preceding frequent US heatwaves in the summer. While our idealized model contains only dry dynamics, the specific structure of climatological state must arise from the substantial contributions of various diabatic processes. On the one hand, local boundary conditions may play an important role on setting up a realistic climatological state. For example, (Donat et al., 2016; Lyon & Dole, 1995; McKinnon et al., 2016) show that the combination of local anomalous sea surface temperature (SST) patterns and atmospheric flow anomalies have contributed significantly to summer extremes. On the other hand, other studies also show the contribution of soil moisture conditions to heat waves by releasing surface diabatic heat (Seneviratne et al., 2010; Miralles et al., 2019) and even to the circumglobal circulation response of Rossby Waves (Douville & Chauvin, 2000; Douville, 2002; Koster et al., 2016). During summer, local land and oceanic conditions are important and may interact nonlinearly with atmospheric circulation states preceding heatwave events. Our next step is to study the dynamics under which local diabatic warming of soil moisture conditions impacts the amplitude of the wave number five pattern and its associated impacts on the statistics of the air temperature extremes in the US.

5 Open Research

The version of the Dry core GCM code used in this work is provided by the open-access data from Wu and Reichler (2018). We construted the target climatology for our simulations from the NCEP-NCAR Reanalysis 1 data provided by the NOAA PSL, Boulder, Colorado, USA. All the NCEP datasets used for this work can be accessed from $https://downloads.psl.noaa.gov/Datasets/ncep.reanalysis/Dailies/$. The temperature at all levels used to construct the inputs for the simulations, and also the velocity fields used for the comparison are in the folder called *pressure/* in that link, and the temperature at 2m in the folder *surface_gauss/*. The data also can be downloaded by following the FTP link in the section Source & References in the NCEP-NCAR Reanalysis 1 webpage: *https://psl.noaa.gov/data/gridded/data.ncep.reanalysis.html*.

The codes for this work and the final datasets obtained from the three simulations are located in the open-access repository *https://github.com/castanev/Dynamics_Heat_Waves.git* linked to Zenodo *DOI*: 10.5281/*zenodo*.7844138

Acknowledgments

The authors acknowledge to NOAA for providing NCEP-NCAR Reanalysis 1 data. They are also grateful to Zheng Wu and Thomas Reichler for providing openly the code of an updated version of the GFDL dry dynamical core GCM.

References

Chang, E. K. M. (2006, July). An Idealized Nonlinear Model of the Northern Hemisphere Winter Storm Tracks. *Journal of the Atmospheric Sciences*, *63*(7), 1818–1839. Retrieved 2023-03-24, from `https://journals.ametsoc.org/view/journals/atsc/63/7/jas3726.1.xml` (Publisher: American Meteorological Society Section: Journal of the Atmospheric Sciences) doi: 10.1175/JAS3726.1

Chen, P., & Newman, M. (1998, October). Rossby Wave Propagation and the Rapid Development of Upper-Level Anomalous Anticyclones during the 1988 U.S. Drought. *Journal of Climate*, *11*(10), 2491–2504. Retrieved 2023-04-07, from `https://journals.ametsoc.org/view/journals/clim/11/10/1520-0442_1998_011_2491_rwpatr_2.0.co_2.xml` (Publisher: American Meteorological Society Section: Journal of Climate) doi: 10.1175/1520-0442(1998)011⟨2491:RWPATR⟩2.0.CO;2

Ding, Q., & Wang, B. (2005, September). Circumglobal Teleconnection in the Northern Hemisphere Summer. *Journal of Climate*, *18*(17), 3483–3505. Retrieved 2023-04-07, from `https://journals.ametsoc.org/view/journals/clim/18/17/jcli3473.1.xml` (Publisher: American Meteorological Society Section: Journal of Climate) doi: 10.1175/JCLI3473.1

Donat, M. G., King, A. D., Overpeck, J. T., Alexander, L. V., Durre, I., & Karoly, D. J. (2016, January). Extraordinary heat during the 1930s US Dust Bowl and associated large-scale conditions. *Climate Dynamics*, *46*(1), 413–426. Retrieved 2023-04-07, from `https://doi.org/10.1007/s00382-015-2590-5` doi: 10.1007/s00382-015-2590-5

Douville, H. (2002, April). Influence of Soil Moisture on the Asian and African Monsoons. Part II: Interannual Variability. *Journal of Climate*, *15*(7), 701–720. Retrieved 2023-04-07, from `https://journals.ametsoc.org/view/journals/clim/15/7/1520-0442_2002_015_0701_iosmot_2.0.co_2.xml` (Publisher: American Meteorological Society Section: Journal of Climate) doi: 10.1175/1520-0442(2002)015⟨0701:IOSMOT⟩2.0.CO;2

Douville, H., & Chauvin, F. (2000, October). Relevance of soil moisture for seasonal climate predictions: a preliminary study. *Climate Dynamics*, *16*(10), 719–736. Retrieved 2023-04-07, from `https://doi.org/10.1007/s003820000080` doi: 10.1007/s003820000080

Feldstein, S. B. (2000, December). The Timescale, Power Spectra, and Climate Noise Properties of Teleconnection Patterns. *Journal of Climate*, *13*(24), 4430–4440. Retrieved 2023-03-31, from `https://journals.ametsoc.org/view/journals/clim/13/24/1520-0442_2000_013_4430_ttpsac_2.0.co_2.xml` (Publisher: American Meteorological Society Section: Journal of Climate) doi: 10.1175/1520-0442(2000)013⟨4430:TTPSAC⟩2.0.CO;2

Fragkoulidis, G., & Wirth, V. (2020, October). Local Rossby Wave Packet Amplitude, Phase Speed, and Group Velocity: Seasonal Variability and Their Role in Temperature Extremes. *Journal of Climate*, *33*(20), 8767–8787. Retrieved 2023-04-07, from https://journals.ametsoc.org/view/journals/clim/33/20/jcliD190377.xml (Publisher: American Meteorological Society Section: Journal of Climate) doi: 10.1175/JCLI-D-19-0377.1

Held, I. M. (2005, November). The Gap between Simulation and Understanding in Climate Modeling. *Bulletin of the American Meteorological Society*, *86*(11), 1609–1614. Retrieved 2023-04-15, from https://journals.ametsoc.org/view/journals/bams/86/11/bams-86-11-1609.xml (Publisher: American Meteorological Society Section: Bulletin of the American Meteorological Society) doi: 10.1175/BAMS-86-11-1609

Held, I. M., & Suarez, M. J. (1994, October). A Proposal for the Intercomparison of the Dynamical Cores of Atmospheric General Circulation Models. *Bulletin of the American Meteorological Society*, *75*(10), 1825–1830. Retrieved 2023-03-24, from https://journals.ametsoc.org/view/journals/bams/75/10/1520-0477_1994_075_1825_apftio_2_0_co_2.xml (Publisher: American Meteorological Society Section: Bulletin of the American Meteorological Society) doi: 10.1175/1520-0477(1994)075⟨1825:APFTIO⟩2.0.CO;2

Hoskins, B. J., & Ambrizzi, T. (1993, June). Rossby Wave Propagation on a Realistic Longitudinally Varying Flow. *Journal of the Atmospheric Sciences*, *50*(12), 1661–1671. Retrieved 2023-04-07, from https://journals.ametsoc.org/view/journals/atsc/50/12/1520-0469_1993_050_1661_rwpoar_2_0_co_2.xml (Publisher: American Meteorological Society Section: Journal of the Atmospheric Sciences) doi: 10.1175/1520-0469(1993)050⟨1661:RWPOAR⟩2.0.CO;2

Jiménez-Esteve, B., & Domeisen, D. I. (2022, July). The role of atmospheric dynamics and large-scale topography in driving heatwaves. *Quarterly Journal of the Royal Meteorological Society*, *148*(746), 2344–2367. Retrieved 2023-04-07, from https://onlinelibrary.wiley.com/doi/10.1002/qj.4306 doi: 10.1002/qj.4306

Koster, R. D., Chang, Y., Wang, H., & Schubert, S. D. (2016, October). Impacts of Local Soil Moisture Anomalies on the Atmospheric Circulation and on Remote Surface Meteorological Fields during Boreal Summer: A Comprehensive Analysis over North America. *Journal of Climate*, *29*(20), 7345–7364. Retrieved 2023-04-07, from https://journals.ametsoc.org/view/journals/clim/29/20/jcli-d-16-0192.1.xml (Publisher: American Meteorological Society Section: Journal of Climate) doi: 10.1175/JCLI-D-16-0192.1

Lyon, B., & Dole, R. M. (1995, June). A Diagnostic Comparison of the 1980 and 1988 U.S. Summer Heat Wave-Droughts. *Journal of Climate*, *8*(6), 1658–1675. Retrieved 2023-04-07, from https://journals.ametsoc.org/view/journals/clim/8/6/1520-0442_1995_008_1658_adcota_2_0_co_2.xml (Publisher: American Meteorological Society Section: Journal of Climate) doi: 10.1175/1520-0442(1995)008⟨1658:ADCOTA⟩2.0.CO;2

McKinnon, K. A., Rhines, A., Tingley, M. P., & Huybers, P. (2016, May). Long-lead predictions of eastern United States hot days from Pacific sea surface temperatures. *Nature Geoscience*, *9*(5), 389–394. Retrieved 2023-04-07, from https://www.nature.com/articles/ngeo2687 (Number: 5 Publisher: Nature Publishing Group) doi: 10.1038/ngeo2687

Meehl, G. A., & Tebaldi, C. (2004, August). More Intense, More Frequent, and Longer Lasting Heat Waves in the 21st Century. *Science*, *305*(5686), 994–997. Retrieved 2023-04-07, from https://www.science.org/doi/10.1126/science.1098704 (Publisher: American Association for the Advancement of Science) doi: 10.1126/science.1098704

Miralles, D. G., Gentine, P., Seneviratne, S. I., & Teuling, A. J. (2019, January). Land–atmospheric feedbacks during droughts and heatwaves: state of the science and current challenges. *Annals of the New York Academy of Sciences*, *1436*(1), 19–35. Retrieved 2023-04-07, from https://www.ncbi.nlm.nih.gov/pmc/articles/PMC6378599/ doi: 10.1111/nyas.13912

Pedlosky, J. (2003). *Waves in the Ocean and Atmosphere: Introduction to Wave Dynamics* (2003rd edition ed.). Berlin ; New York: Springer.

Röthlisberger, M., Frossard, L., Bosart, L. F., Keyser, D., & Martius, O. (2019, June). Recurrent Synoptic-Scale Rossby Wave Patterns and Their Effect on the Persistence of Cold and Hot Spells. *Journal of Climate*, *32*(11), 3207–3226. Retrieved 2023-04-07, from https://journals.ametsoc.org/view/journals/clim/32/11/jcli-d-18-0664.1.xml doi: 10.1175/JCLI-D-18-0664.1

Schubert, S., Wang, H., & Suarez, M. (2011, September). Warm Season Subseasonal Variability and Climate Extremes in the Northern Hemisphere: The Role of Stationary Rossby Waves. *Journal of Climate*, *24*(18), 4773–4792. Retrieved 2023-04-15, from https://journals.ametsoc.org/view/journals/clim/24/18/jcli-d-10-05035.1.xml (Publisher: American Meteorological Society Section: Journal of Climate) doi: 10.1175/JCLI-D-10-05035.1

Seneviratne, S. I., Corti, T., Davin, E. L., Hirschi, M., Jaeger, E. B., Lehner, I., ... Teuling, A. J. (2010, May). Investigating soil moisture–climate interactions in a changing climate: A review. *Earth-Science Reviews*, *99*(3), 125–161. Retrieved 2023-04-15, from https://www.sciencedirect.com/science/article/pii/S0012825210000139 doi: 10.1016/j.earscirev.2010.02.004

Teng, H., Branstator, G., Wang, H., Meehl, G. A., & Washington, W. M. (2013, December). Probability of US heat waves affected by a subseasonal planetary wave pattern. *Nature Geoscience*, *6*(12), 1056–1061. Retrieved 2023-03-24, from https://www.nature.com/articles/ngeo1988 (Number: 12 Publisher: Nature Publishing Group) doi: 10.1038/ngeo1988

Vallis, G. K. (2017). *Atmospheric and Oceanic Fluid Dynamics: Fundamentals and Large-Scale Circulation* (2nd ed.). Cambridge: Cambridge University Press. Retrieved 2023-03-01, from https://www.cambridge.org/core/books/atmospheric-and-oceanic-fluid-dynamics/41379BDDC4257CBE11143C466F6428A4 doi: 10.1017/9781107588417

Wirth, V., Riemer, M., Chang, E. K. M., & Martius, O. (2018, July). Rossby Wave Packets on the Midlatitude Waveguide—A Review. *Monthly Weather Review*, *146*(7), 1965–2001. Retrieved 2023-04-05, from https://journals.ametsoc.org/view/journals/mwre/146/7/mwr-d-16-0483.1.xml (Publisher: American Meteorological Society Section: Monthly Weather Review) doi: 10.1175/MWR-D-16-0483.1

Wu, Z., & Reichler, T. (2018). Towards a more earth-like circulation in idealized models. Retrieved from https://doi.org/ doi: 10.1029/2018MS001356

Zimin, A. V., Szunyogh, I., Patil, D. J., Hunt, B. R., & Ott, E. (2003, May). Extracting Envelopes of Rossby Wave Packets. *Monthly Weather Review*, *131*(5), 1011–1017. Retrieved 2023-03-24, from https://journals.ametsoc.org/view/journals/mwre/131/5/1520-0493_2003_131_1011_eeorwp_2.0.co_2.xml (Publisher: American Meteorological Society Section: Monthly Weather Review) doi: 10.1175/1520-0493(2003)131⟨1011:EEORWP⟩2.0.CO;2

Supporting Information for "The Role of Climatological State on Driving US Heat Waves Through Rossby Waves Packets"

Valentina Castañeda[1], Lei Wang[1]

[1]Department of Earth, Atmospheric, and Planetary Sciences, Purdue University

Contents of this file

1. Description of the Dry Core GCM
2. Figures S1 to S2

Introduction

This document includes a more detailed description of the model used for the three simulations in this work. In addition, two figures with a comparison of the climatological state between the experiments and the reanalysis data.

1. Description of the Dry Core GCM

Idealized general circulation models are commonly used for the study of atmospheric dynamics. This kind of models solve the primitive equations by nudging the temperature toward a prescribed equilibrium temperatures (T_{eq}). Essentially, this process isolates the dynamics from the complex physical parametrizations. However, as the primitive equations are solved on the sphere, there is some confidence that large-scale dynamics relate to the real atmosphere. In this work, we use the open-access updated version from (Wu & Reichler, 2018) of the spectral dynamical core model proposed by (Held & Suarez, 1994) for the Geophysical Fluid Dynamics Laboratory (GFDL).

The model has horizontal resolution of T42 (64x128 grid) and 40 vertical σ levels between the surface and 0.01 hPa. Rayleigh drag with a prescribed rate, which decreases linearly with height from a surface value k_f to zero at ($\sigma = 0.7$) and higher levels, is used to remove momentum from the low levels, representing the boundary-layer friction. Mathematically, this can be written by:

$$\frac{\partial v}{\partial t} = ... - k_v(\sigma)v \tag{1}$$

Where v represents the wind and σ the vertical sigma level. The damping rate (k_v) follows the form:

$$k_v = k_f max\left(0, \frac{\sigma - \sigma_b}{1 - \sigma_b}\right) \tag{2}$$

where $k_f = 1day^{-1}$ and $\sigma_b = 0.7$ is the vertical level in the model where the top of the boundary layer is defined. The temperature is forced by Newtonian relaxation toward a prescribed equilibrium temperature as follows:

$$\frac{\partial T}{\partial t} = \frac{T - T_{eq}}{\tau} \tag{3}$$

where τ is the prescribed relaxation timescale following the distribution:

$$\tau^{-1} = k_a + (k_s - k_a) max \left(0, \frac{\sigma - \sigma_b}{1 - \sigma_b}\right) cos^4\phi \tag{4}$$

where $k_a = 1/40\ day^{-1}$ and $k_s = 1/4\ day^{-1}$ are parameters to set the distribution of the relaxation coeficient. In this model, the T_{eq} is zonally symmetric and is easily set through parameters. Since the primary purpose of this study is to examine how the atmospheric basic state controls the pattern contained in Rossby Waves driving heat waves, the model includes the iterative procedure proposed by (Chang, 2006) to simulate the climatological basic state of the atmosphere in the idealized model. This consists of iterating the radiative equilibrium temperature profile so that at the end of the iterations, the model climate closely resembles the desired target climate. The iteration uses a fixed equilibrium temperature for each N step (T_{eq}) in a run of Y years. Then, we calculate the model simulated temperature climatology $T_{(N)}$ and correct it concerning basic state from the NCEP reanalysis data T_R. The next iteration step N+1 is calculated according to:

$$T_{eq(N+1)} = T_{eq(N)} - \frac{2}{3}(T_{(N)} - T_R), N = 1, 2, 3... \tag{5}$$

References

Chang, E. K. M. (2006, July). An Idealized Nonlinear Model of the Northern Hemisphere Winter Storm Tracks. *Journal of the Atmospheric Sciences*, *63*(7), 1818–1839. Retrieved 2023-03-24, from `https://journals.ametsoc.org/view/journals/atsc/63/7/jas3726.1.xml` (Publisher: American Meteorological Society Section: Journal of the Atmospheric Sciences) doi: 10.1175/JAS3726.1

Held, I. M., & Suarez, M. J. (1994, October). A Proposal for the Intercomparison of the Dynamical Cores of Atmospheric General Circulation Models. *Bulletin of the American Meteorological Society*, *75*(10), 1825–1830. Retrieved 2023-03-24, from https://journals.ametsoc.org/view/journals/bams/75/10/1520-0477_1994_075_1825_apftio_2_0_co_2.xml (Publisher: American Meteorological Society Section: Bulletin of the American Meteorological Society) doi: 10.1175/1520-0477(1994)075⟨1825:APFTIO⟩2.0.CO;2

Wu, Z., & Reichler, T. (2018). Towards a more earth-like circulation in idealized models. Retrieved from https://doi.org/ doi: 10.1029/2018MS001356

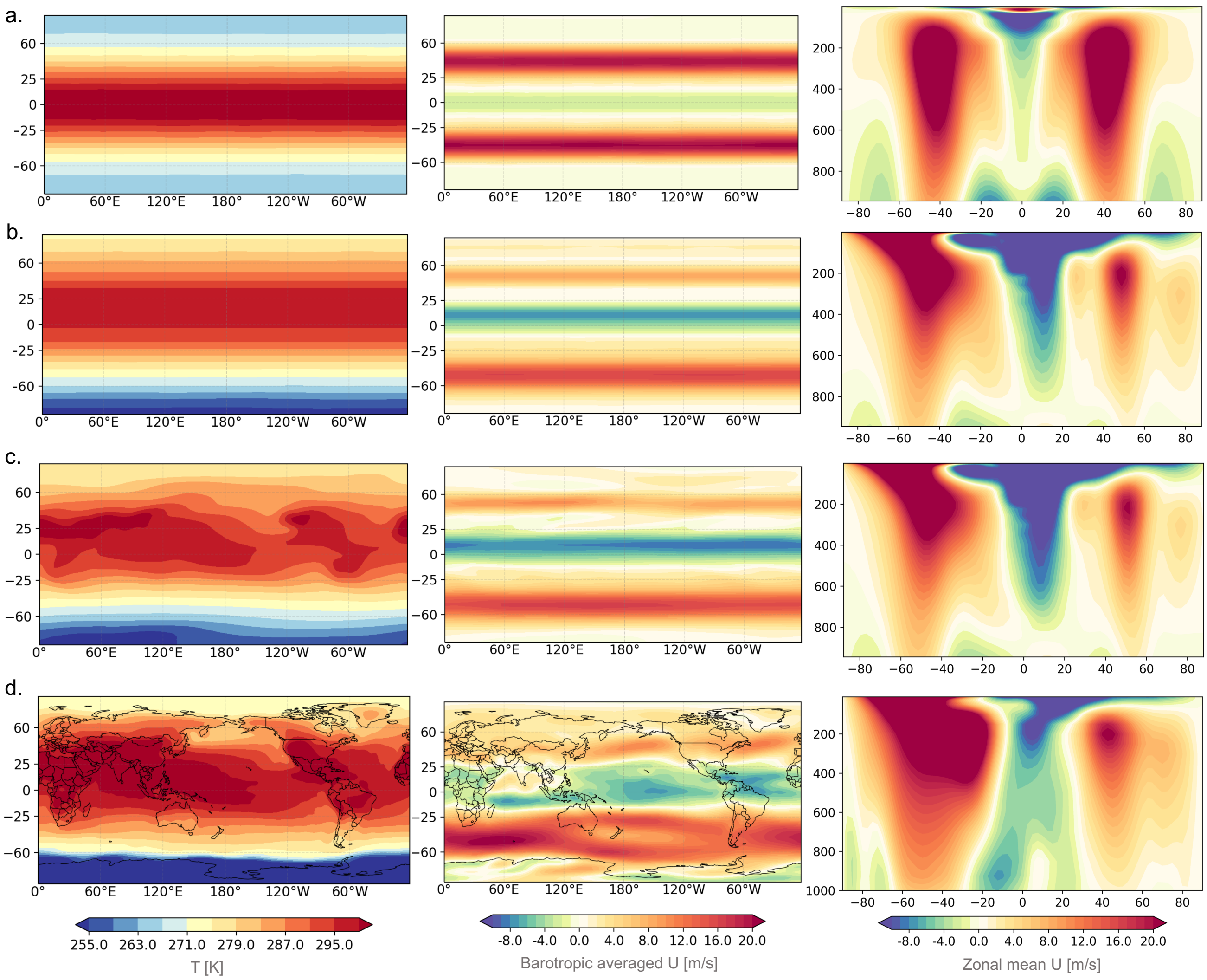

Figure S1. Basic state of the surface air temperature (SAT) (left column), the barotropic averaged zonal wind (middle column) and the vertical distribution of the zonal wind (right column) for the Held and Suarez 1994 (exp1_HS94) experiment (a.), the bias corrected experiment with the symmetrical SAT from NCEP (b.), the bias corrected experiment with the asymmetrical SAT from NCEP (c.) and NCEP (d.).

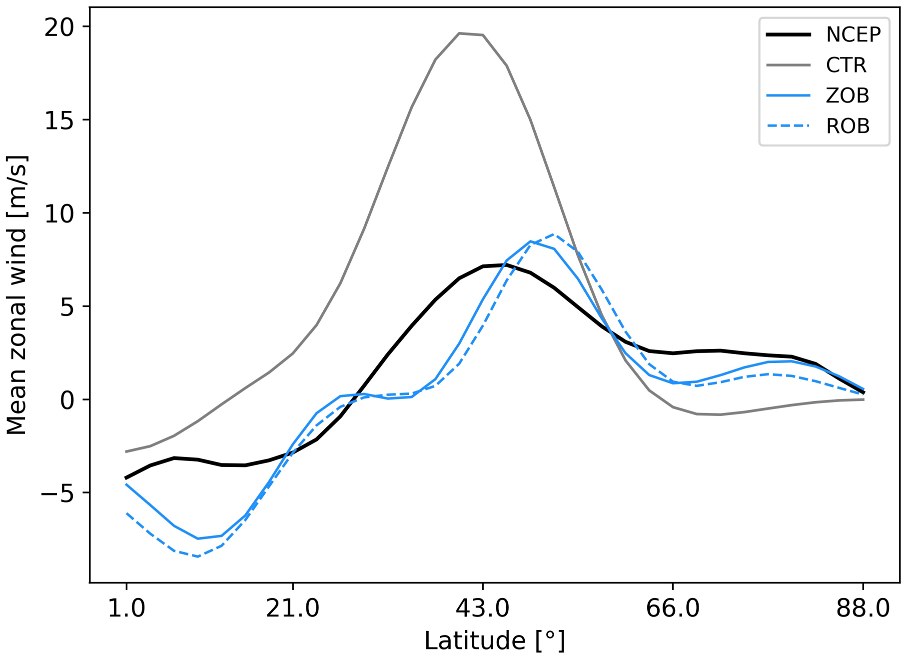

Figure S2. Comparison of the barotropic zonal mean zonal wind between NCEP, the Held and Suarez 1994 (exp1_HS94) experiment and the bias corrected experiments.